LIMNOLOGY
and
OCEANOGRAPHY

ASLO

Limnol. Oceanogr. 00, 2015, 00–00

doi: 10.1002/lno.10228

Climate change impacts on lake thermal dynamics and ecosystem vulnerabilities

G. B. Sahoo,*[1,2] A. L. Forrest,[1,3] S. G. Schladow,[1,2] J. E. Reuter,[1] R. Coats,[1] M. Dettinger[4]

[1]Tahoe Environmental Research Center, UC Davis, Davis, California
[2]Department of Civil and Environmental Engineering, UC Davis, Davis, California
[3]Australian Maritime College, University of Tasmania, Launceston, Tasmania, Australia
[4]US Geological Survey and Scripps Institution of Oceanography, La Jolla, California

Abstract

Using water column temperature records collected since 1968, we analyzed the impacts of climate change on thermal properties, stability intensity, length of stratification, and deep mixing dynamics of Lake Tahoe using a modified stability index (SI). This new SI is easier to produce and is a more informative measure of deep lake stability than commonly used stability indices. The annual average SI increased at 16.62 kg/m^2/decade although the summer (May–October) average SI increased at a higher rate (25.42 kg/m^2/decade) during the period 1968–2014. This resulted in the lengthening of the stratification season by approximately 24 d. We simulated the lake thermal structure over a future 100 yr period using a lake hydrodynamic model driven by statistically downscaled outputs of the Geophysical Fluid Dynamics Laboratory Model (GFDL) for two different green house gas emission scenarios (the A2 in which greenhouse-gas emissions increase rapidly throughout the 21st Century, and the B1 in which emissions slow and then level off by the late 21st Century). The results suggest a continuation and intensification of the already observed trends. The length of stratification duration and the annual average lake stability are projected to increase by 38 d and 12 d and 30.25 kg/m^2/decade and 8.66 kg/m^2/decade, respectively for GFDLA2 and GFDLB1, respectively during 2014–2098. The consequences of this change bear the hallmarks of climate change induced lake warming and possible exacerbation of existing water quality, quantity and ecosystem changes. The developed methodology could be extended and applied to other lakes as a tool to predict changes in stratification and mixing dynamics.

Changes in the mixing dynamics of lakes depend on heating, cooling, mixing, and circulation patterns. In turn, each of these processes is highly dependent on regional and global climatic variability. Analysis of historic hydroclimatic data shows increasing air temperature resulting in increasing lake water temperature, which is the key parameter to alter ecosystem dynamics and services (Coats et al. 2006; Coats 2010; Sahoo et al. 2011). Climate change is expected to continue or even accelerate the increasing trends air and water temperature under near-future climatic conditions as projected by global climate models (IPCC 2007; U.S. Global Change Research Program 2009; Dufresne et al. 2013; Koenigk et al. 2013). Therefore, quantification of climate-induced changes in lake physics is required to devise management plans for our freshwater resources and to address ecosystem adaptation to climate change (Sahoo and Schladow 2008). This study describes the types and possible magnitudes of deep-water lake responses to climate change.

Resistance to mixing across the thermocline increases markedly even at a temperature gradients of only a few degrees. In this context, the measured and modeled trends of increased intensity and duration of surface stratification and reduced deep mixing to lake bottom (up to 500 m) in Lake Tahoe (linked to projected climate changes), documented here, raise the specter of new avenues of ecosystem vulnerabilities. In Lake Tahoe, the vertical partitioning of the water column during summer stratification suppresses mixing between the nutrient enriched hypolimnion and the nutrient poor epilimnion (Paerl et al. 1975). A change in mixing properties and depth of deep mixing can have significant consequences on nutrient supply to the upper waters, thereby affecting primary productive and food-web dynamics. In addition, should deep mixing be curtailed, the

Additional Supporting Information may be found in the online version of this article.

*Correspondence: gbsahoo@ucdavis.edu

potential for deep-water anoxia would have very serious consequences on the resident salmonid populations.

In a recent modeling study of Lake Tahoe mixing using regionally downscaled output for key meteorological forcing factors in the 21st Century (Dettinger 2013), Sahoo et al. (2013a) reported it very possible that Lake Tahoe could cease to mix to the bottom after about 2060 for the GFDL A2 future climate scenario, with a mixing depth of less than 200 m. Deep mixing, which currently occurs on average every 3–4 yr, will (under the GFDL B1 scenario) occur only four times between 2060 and the end of the 21st Century. It is hypothesized that, if the lake fails to completely mix for over 6 yr in a row, the hypolimnetic dissolved oxygen concentration will be depleted to zero (Sahoo et al. 2013a). When this occurs, orthophosphate and ammonium (both biostimulatory) are released from the deep sediments, raising the possibility of future algal blooms.

Stability indices are used to measure lake resistance to mixing and include: Brunt–Väisälä frequency (N^2); and Thermocline Strength Index (TSI) (Yu et al. 2010); the relative thermal resistance (RTR) (Vallentyne 1957); the Schmidt Stability Index (SSI) (Schmidt 1928; Idso 1973); and the Hutchinson's stability index (SI) (Hutchinson 1957). More commonly used stability indices, such as N^2, TSI, and RTR measure local stability, i.e., not for the entire water column; whereas SSI and Hutchinson's SI quantify the stability of the entire water column. However, surface water temperatures exhibit a rapid and direct response to climatic forcing in contrast to hypolimnetic temperatures that exhibit a much more complex behavior, making epilimnetic temperature a potentially better indicator of climate change.

In this article, we evaluate a long-term dataset (1968–2014) for trends in lake thermal properties, the length of the stratification period, and stratification intensity for Lake Tahoe using a newly developed simple SI that measures the stratification intensity and duration in the upper 100 m of the water column of the lake. Specific objectives of this study were to: (1) develop a simpler SI, (2) estimate stratification intensity and duration trends using the 47-yr record, (3) apply the developed SI to evaluate stratification duration and intensity of the 21st Century using modeled water temperature for Lake Tahoe (Sahoo et al. 2013a) and (4) discuss the consequences of the predicted future stratification conditions in terms of lake water quality, water quantity and ecosystem function.

Study area

Lake Tahoe is renowned for its extraordinary deep-water transparency. The maximum and average depths of the lake are 500 m and 305 m. The basin consists of one outflow tributary and a total of 63 inflow tributaries that drain approximately 12×10^6 m^3/yr flow (average of 1994–2008) into the lake from the surrounding watershed (Sahoo et al. 2013b). As the ratio of the lake watershed area (813 km^2) to the lake surface area (501 km^2) is only 1.62, and the total volume of the lake is 158 km^3, the mean hydraulic residence time is 650–700 yr.

As a result of Lake Tahoe's large depth and volume, the water column stores much of the shortwave radiation striking the lake surface during spring and summer and releases it as latent and sensible heat and longwave radiation during winter (Sahoo et al. 2013b). Lake Tahoe never has complete continuous ice-cover and is described as warm-monomictic. Long-term data since 1968 show that the deepest mixing typically occurs in the period of February–March and that complete mixing occurs once in every 3–4 yr on average (Tahoe Environmental Research Center (TERC) 2015). Lake Tahoe stratifies in the upper 100 m with seasonally warmer water in the epilimnion overlying hypolimnetic waters, which remain at around 5°C. Summer (June–October) warming establishes a stable thermocline at a depth of approximately 20 m. As the lake cools in the fall, the thermocline typically lowers and by end of October is at a depth of approximately 30–40 m. Complete mixing to 500 m, if it occurs, usually happens in March.

Lake Tahoe has been studied intensively with continuous meteorological records spanning over 100 yr. Previous work on the historic trends in the basin's hydroclimatology (1910–2007) indicated strong upward trends in air temperature (especially night-time temperature), a shift from snowfall to rainfall, a shift in snowmelt timing to earlier dates, increased rainfall intensity, increased interannual variability and an increase in the temperature of Lake Tahoe (Coats et al. 2006; Coats 2010; Sahoo et al. 2011).

Methodology

The following methods offer approaches for calculating two of the more common lake-specific indices for stratification, including buoyancy frequency (N) and SSI. In addition, our simplified SI is presented. In this study, the air/water interface has a zero depth and the downward direction in the z-axis is considered to be positive.

Buoyancy frequency (N)

The buoyancy frequency is often called the Brunt–Väisälä frequency or the stratification frequency. This index measures resistance to turbulence, in inverse time units. The frequency can be physically interpreted as the vertical frequency excited by a vertical displacement of a fluid parcel and is estimated using Eq. 1.

$$N = \sqrt{\frac{g}{\rho_z}\frac{\partial \rho_z}{\partial z}} \tag{1}$$

where N represents the local stability of the water column, based on the vertical density gradient $\partial\rho/\partial z$, g is the acceleration due to gravity, and ρ_z is the density at depth z. We estimated lake water density using methods described in Millero et al. (1980), Chen and Millero (1986) and Pawlowicz (2008) (see Supporting Information).

Schmidt's stability index (SSI)

The SSI of a lake is an estimate of the idealized amount of energy required to mix the entire lake to a uniform temperature over the depth of the water column without the addition or subtraction of heat (Schmidt 1915, 1928). Idso (1973) modified the original proposed SSI to reduce lake volume effects and normalize the required mixing energy per unit area. Various authors (e.g., Coats et al. 2006; Yu et al. 2010; Read et al. 2011) have adopted Idso's methodology. Calculation of Idso's modified SSI is based on the comparison between the measured vertical center of mass of a stratified lake as compared with the vertical location of the completely mixing lake defined by Eq. 2.

$$\mathrm{SSI} = \frac{g}{A_0} \sum_{z_0}^{z_m} \left(z - z_{\overline{\rho}}\right)\left(\rho_z - \overline{\rho}\right) A_z \Delta z \quad (\mathrm{J/m^2}) \tag{2}$$

where A_0 is the lake surface area, $\bar{\rho}$ is the mean density, $z\bar{\rho}$ is the depth where the mean density is found (depth to the center of gravity of the lake), A_z is the area at depth z, z_0 is the water surface depth, z_m is the maximum depth, Δz is the layer thickness, $A_z \times \Delta z$ is the volume of the layer. The center of mass (CM) $z\bar{\rho}$ and mean density ($\bar{\rho}$) are estimated using Eqs. 3 and 4, respectively.

$$z\bar{\rho} = \frac{1}{\sum_{z_0}^{z_m} \rho_z A_z \Delta z} \sum_{z_0}^{z_m} \rho_z z A_z \Delta z \tag{3}$$

$$\bar{\rho} = \frac{1}{\sum_{z_0}^{z_m} A_z \Delta z} \sum_{z_0}^{z_m} \rho_z A_z \Delta z \tag{4}$$

Stability index (SI)

Adrian et al. (2009) demonstrated that surface water temperatures exhibit a rapid and direct response to climatic forcing in contrast to hypolimnetic temperatures that exhibit a much more complex behavior, making epilimnetic temperature a useful indicator of climate change. The disadvantage of the using the SSI for very deep lakes is that the rest of the water column overwhelms variations in stability of the upper water column. As stratification in Lake Tahoe is observed in the upper 100 m and the surface area of the whole-lake layers at these depths is relatively uniform (A_z from Eq. 2), it is proposed to use a simple SI that measures the energy required to mix the lake when it is stratified using Eq. 5.

$$\mathrm{SI} = \sum_{z=z_0}^{z=z_1} (z - \bar{z})\rho_z \tag{5}$$

Here z is the depth of the water column from the surface, and z_0, z_1, and $\bar{z}$ are the depths of the surface water, the lower end of the water column, and the centroid of the water column, respectively. Water density at depth z is ρ_z. The SI can be converted to energy by multiplying by the gravitational acceleration and each layer volume, these are all constant as described above.

Required data

Water temperature and water quality data in the lake are monitored regularly at two stations: (1) Lake Tahoe Profile (LTP) located along the west shore albeit with a depth of approximately 160 m and (2) Mid-Lake Tahoe Profile (MLTP) in the deeper part of the lake (460 m deep). Lake Tahoe water temperature profiles at LTP and MLTP are available since 1968. Since water temperature measurements employed reversing thermometers for the period 1968–2005, water temperature profiles collected at the LTP station include data points at every 3 m depth; however, most of the water temperature profiles at MLTP station include data points at depths of 0 m (surface), 10 m, 50 m, 100 m, 150 m, 200 m, 250 m, 300 m, 350 m, 400 m, and 450 m. Since 2005, water temperature profiles have been measured using Seabird CTDs (Seabird Electronics); approximately 1–160 m at the LTP and approximately 1–460 m at the MLTP. Depending at the rate of fall, Seabird instruments measures water temperatures at approximately 0.2 m intervals starting from 1 m. To estimate lake SI, water temperature profiles during 1968–2005 were linearly interpolated between depth readings to get the data from surface (0 m) to 100 m at 1 m intervals (0, 1, 2, . . ., 100). In this study, we used the temperature and conductivity Seabird profiles bin average in the vertical at 1 m bins.

Jassby et al. (1999) reported that water quality data from the two stations exhibit self-consistent patterns of variation. Field data from these two stations show much more variation along the vertical plane than on the horizontal, justifying the use of the data of either station as the basis for SI estimates. Since temperature profiles have been measured approximately every 10 d at LTP station and once a month at MLTP station and lake stratification occurs in the upper 100 m, we used the lake water temperature data of LTP station in our calculations. We used the lake hypsographic information (the surface area and cumulative volume as functions of elevation) as reported in Gardner et al. (1998).

Statistical analysis

Significance (Mann-Kendall p-value) is based on the normal probability distribution of data over time and is estimated by non-parametric linear regression analysis. If the Mann-Kendall p-value is greater than 0.1 (10%), we considered that there is no meaningful existing temporal trend in the dataset.

Effect of continued warming

Sahoo et al. (2013a) estimated Lake Tahoe water temperature using the Dynamic Lake Model with Water Quality (DLM-WQ) and spatially downscaled meteorology data (air temperature, precipitation, wind speed, longwave radiation, and solar radiation) during the 21st Century. The spatially statistically downscaled meteorology data were obtained from

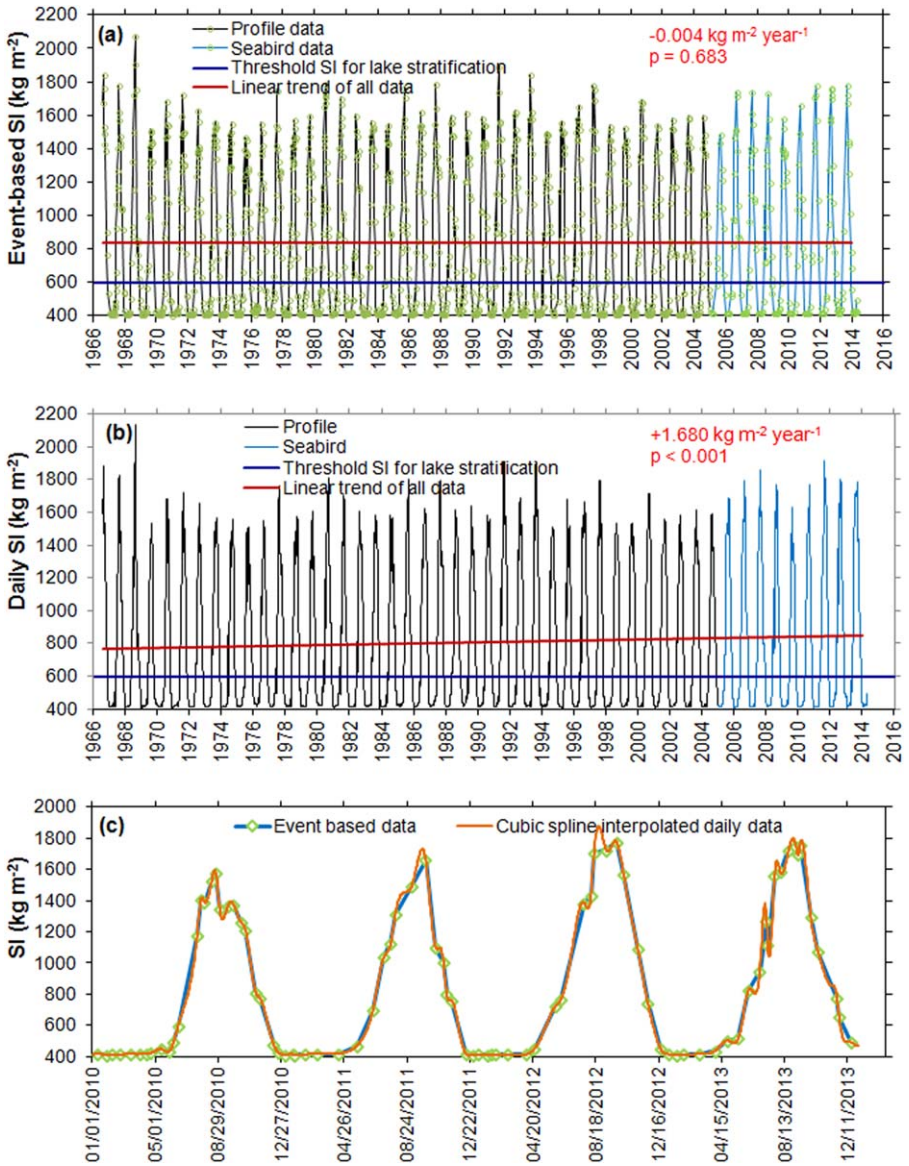

Fig. 1. (**a**) Event-based SI, (**b**) daily SI, and (**c**) comparison between event-based and interpolated daily SI. The blue and red lines show the threshold SI for lake stratification and linear trend using all data, respectively. The symbols "+" and "−"in red texts represent increasing and decreasing trend, respectively. *X*-axis values in (**a**) and (**b**) represent the beginning of the year. [Color figure can be viewed in the online issue, which is available at wileyonlinelibrary.com.]

the coarse grid meteorological output of the Geophysical Fluid Dynamics Laboratory Model (GFDL CM2.1) (Delworth et al. 2006) for the A2 and B1 Special Report on Emissions Scenarios (SRES) reported by the Intergovernmental Panel on Climate Change (IPCC) (Dettinger 2013). The A2 is (the revised IPCC fifth Assessment Report (AR5) (2014) defined Representative Concentration Pathways (RCP) 8.5 was based on the SRES A2) an emissions scenario developed by the Intergovernmental Panel on Climate Change (IPCC) in 2001 in which greenhouse-gas emissions increase rapidly throughout the 21st Century, and the B1 (the revised RCP4.5 was based on the SRES B1) is a more moderate scenario in which emissions slow and then level off by the late 21st Century. In these scenarios, annual air temperatures at Lake Tahoe are projected to increase by an additional 2–4.5°C by the year 2100 (Sahoo et al. 2013a). In addition, longwave radiation is projected to increase by approximately 5–10% and wind speeds to decline on the order of 7–10% (Sahoo et al. 2013a).

Daily and event-based lake SI

The event-based lake SI for 1968–2014 in Fig. 1 shows that lake stratification starts in June, peaks in October and ends in November. The length of stratification period in a given year is the difference between the dates of onset and

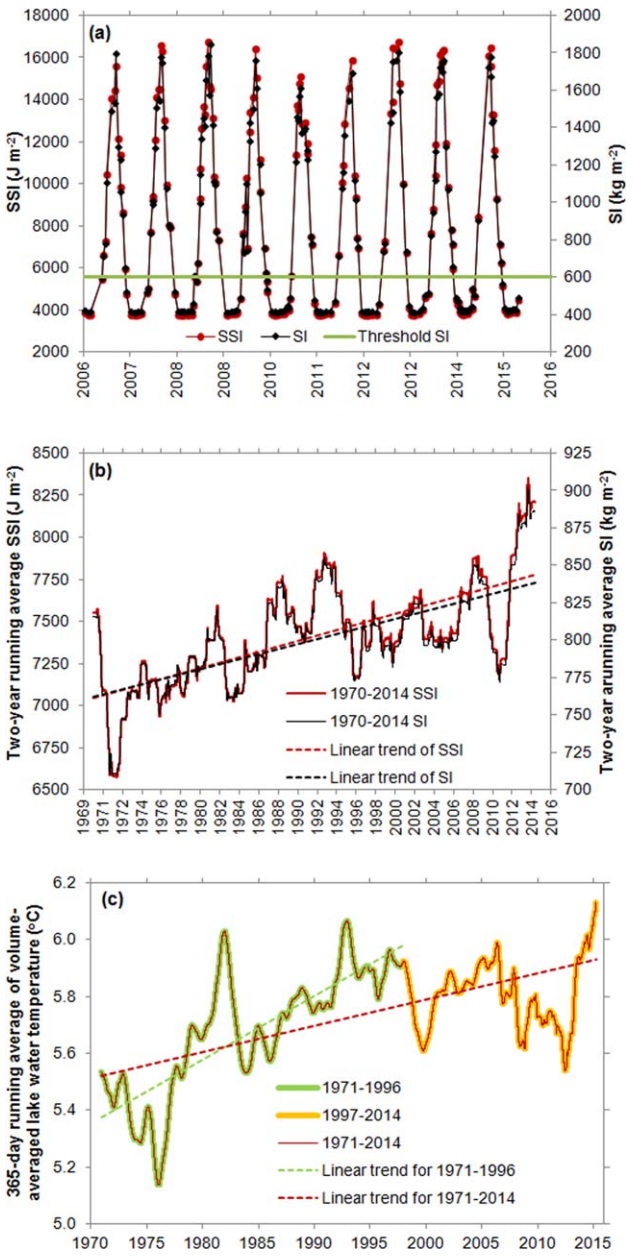

Fig. 2. (**a**) SSI and SI using event based seabird data during 2006–2014. (**b**) 2-yr running average SSI and SI using interpolated daily data during 1968–2014. (**c**) 365-d running average of volume-averaged lake water temperature using interpolated daily data during 1970–2014. [Color figure can be viewed in the online issue, which is available at wileyonlinelibrary.com.]

end of a stratified water column. Although Fig. 1a produces the general trend of the stratification period, estimation of the stratification period from event-based dataset alone includes bias because it depends on the date of measurements. Event measurements often yield abrupt changes in SI, complicating estimation of stratification periods between two measurements and are not a true representation of the system as lake water temperatures and stratification evolve smoothly over the annual heating cycle (Sahoo et al. 2010, 2013b).

To minimize bias in the estimation of the stratification period, temperature and conductivity profiles are interpolated between the event-based dates using the MATLAB cubic spline function. Lake SI values in Fig. 1b are estimated using the interpolated daily temperature and conductivity profiles and the density calculations detailed previously. Figure 1c illustrates that event-based SI values and interpolated SI values overlap each other. Although Fig. 1a looks similar to Fig. 1b, there is significant difference in observed trends. The linear regression line in Fig. 1a shows a decreasing trend at −0.40 kg/m^2/decade with very poor statistical correlation significance value (Mann-Kendall p-value = 0.683) whereas the linear regression line in Fig. 1b shows an increasing trend at 16.80 kg/m^2/decade with a very strong statistical correlation significance value (Mann-Kendall p-value < 0.001). Such differences are observed because of paucity of data in event-based case to represent physical processes and lake dynamics. The presence of insufficient number of data points in Fig. 1a skewed the linear trend. Since the interpolated daily lake SI values are more meaningful to represent the physical processes and have strong correlation, we used these data for the lake annual and seasonal stability and stratification period analysis.

Results

Annual and seasonal lake stability

The values of SSI (J/m^2) and SI (kg/m^2) using event based Seabird data during 2006–2014 are compared in Fig. 2a. The trend of event based SI follows closely to that of SSI justifying use of SI to measure stratification intensity and duration of Lake Tahoe. Figure 2b shows 2-yr running average SSI and SI using interpolated daily data during 1970–2014. To smooth seasonal variations and to show the long-term trend, the 2-yr running average SSI and SI values are presented for the lake. The trend of the 2-yr running average daily SI follows closely that of SSI. The SSI and SI represent the amount of work required by the destabilizing energy from thermal convection and surface wind shear for a water column to overcome thermal stratification for mixing. SSI and SI have increased by approximately 726 J/m^2 and 76 kg/m^2, respectively since 1970 at a rate of 16.510 J/m^2/yr and 1.718 kg/m^2/yr, respectively (Mann-Kendall p-value < 0.00001). Thus, there should be a reduction in mixing with increasing SSI and SI. Although Fig. 2b shows the general increasing trend of SSI and SS, it is evident that the lake stability increased at higher rate until the end of 1996 as compared with the period between 1997 and 2011. This is consistent with the trend of volume weighted lake water temperature shown in Fig. 2c.

The annual average lake SI (kg/m^2) in Fig. 3a shows that there has been an overall increase in lake stability at 1.662 kg/m^2/yr with very strong statistical correlation

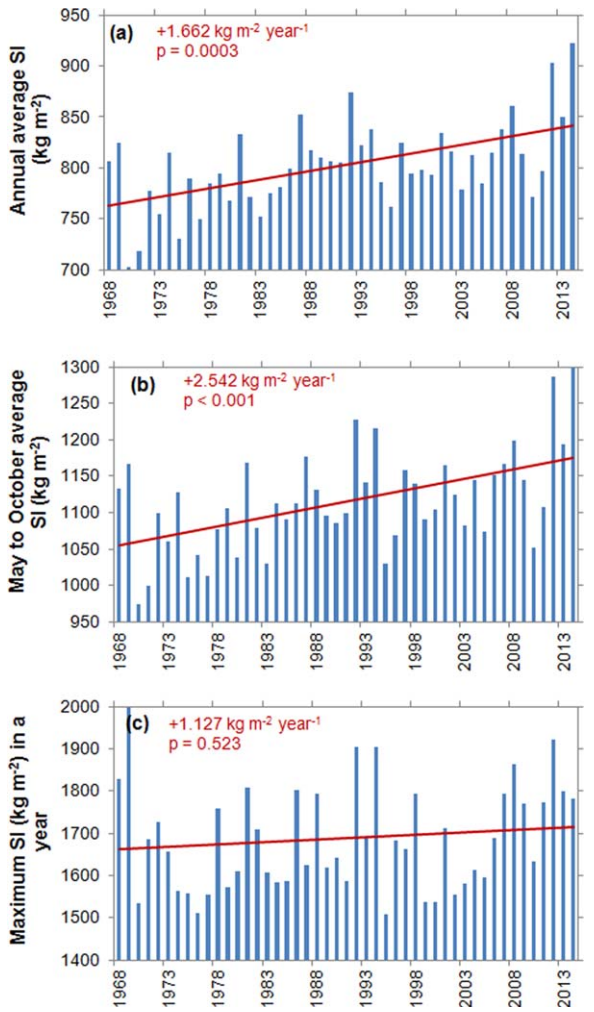

Fig. 3. (**a**) Annual average SI (kg m^{-2}) in a year, (**b**) summer (May–October) average SI (kg m^{-2}), and (**c**) the peak SI (kg m^{-2}) in a year during 1968–2014. The red line shows the linear trend. The symbols "+" and "−"in red texts represent increasing and decreasing trend, respectively. [Color figure can be viewed in the online issue, which is available at wileyonlinelibrary.com.]

significance value (Mann-Kendall p-value = 0.0003) between 1968 and 2014. An increasing trend is also found over the same period of record for the summer (May–October) average lake SI (Fig. 3b) data, albeit at a higher rate (i.e., 2.542 kg/m^2/yr with very strong statistical correlation significance value (Mann-Kendall p-value < 0.001)). Peak annual lake SI (kg/m^2) (Fig. 3c) increased at a minimal rate (i.e., 1.127 kg/m^2/yr) and was not statistically significant (Mann-Kendall p-value = 0.523). Similar to the annual average lake SI, the 2014 summer (May–October) average lake SI was found to be high. However, Fig. 3c shows that peak SI in year 2014 is not an all time high. This clearly indicates that the longer stratification season in 2014 is the cause of the all-time high annual average lake SI and the summer average lake SI.

Lake stratification season

The running average SSI and SI trends of the lake stability show a lake warming trend although they are not the proper metrics to show detailed changes in lake stratification pattern and stability intensity and pattern over time. The greater value of buoyancy frequency (N) coincides with the steeper density gradient (i.e., the thermocline). ΣN indicates total stratification intensity and peak N identifies the location of the thermocline (Fig. 4). The ΣN was larger for higher stratification intensity and width of thermocline (e.g., profiles of 27 July 2010 and 25 August 2010). The SI value depends on both the width of the metalimnion and stratification intensity. For example, maximum N, the width of the metalimnion, and SI on 11 January 2010 are 0.007 Hz, negligible and 418 kg/m^2, respectively while maximum N, the width of the metalimnion, and SI on 27 July 2010 are 0.07 Hz, approximately 60 m and 1406 kg/m^2, respectively. It is evident in Fig. 4 that the lake stratifies at a peak N greater than approximately 0.015 Hz.

Figures 4, 5 show that there are no peaks around SI 600 kg/m^2 suggesting that Lake Tahoe is monomictic and that there is one stratification season. Comparison of lake SI and buoyancy frequency of two different years (1971 and 2008) in Fig. 5 illustrates that not only have the lake SI and buoyancy frequency values increased significantly but also the length of the stratification season has increased mostly as a result of delay in the onset of winter. The beginning and the end dates of the stratification season have shifted to earlier and later dates, respectively. Figures 2a, 4 illustrate that the lake strongly stratifies for SI greater than approximately 600 kg/m^2, which requires higher destabilizing energy from thermal convection, lower shortwave radiation, lower air temperature, and surface wind shear for erosion and deepening of the thermocline. In the present analysis, lake stratification is taken to begin on the day when the SI exceeds 600 kg/m^2 and end on the day when the SI falls below 600 kg/m^2. The length of stratification period in a given year is the difference between the last Julian and first Julian date with stratification.

The trends of length of stratification season, beginning of the stratification season, end of the stratification season and peak stratification day in a year during 1968–2014 are analyzed in Figures 6a, 7. Consistent with Fig. 5, the length of stratification season has increased approximately 24 d (Mann-Kendall p-value = 0.005) (Fig. 6a) in the past 47 yr (1968–2014). The beginning of the stratification season has shifted to 5 d earlier (Mann-Kendall p-value = 0.287) (Fig. 7) while the end of the stratification season has delayed to 19 d (Mann-Kendall p-value = 0.005) (Fig. 7) due to delay in the onset of winter mixing. Although the stratification season has increased by approximately 24 d, the peak stratification day in a year has shifted to only 5 d later, an insignificant change (Mann-Kendall p-value = 0.692).

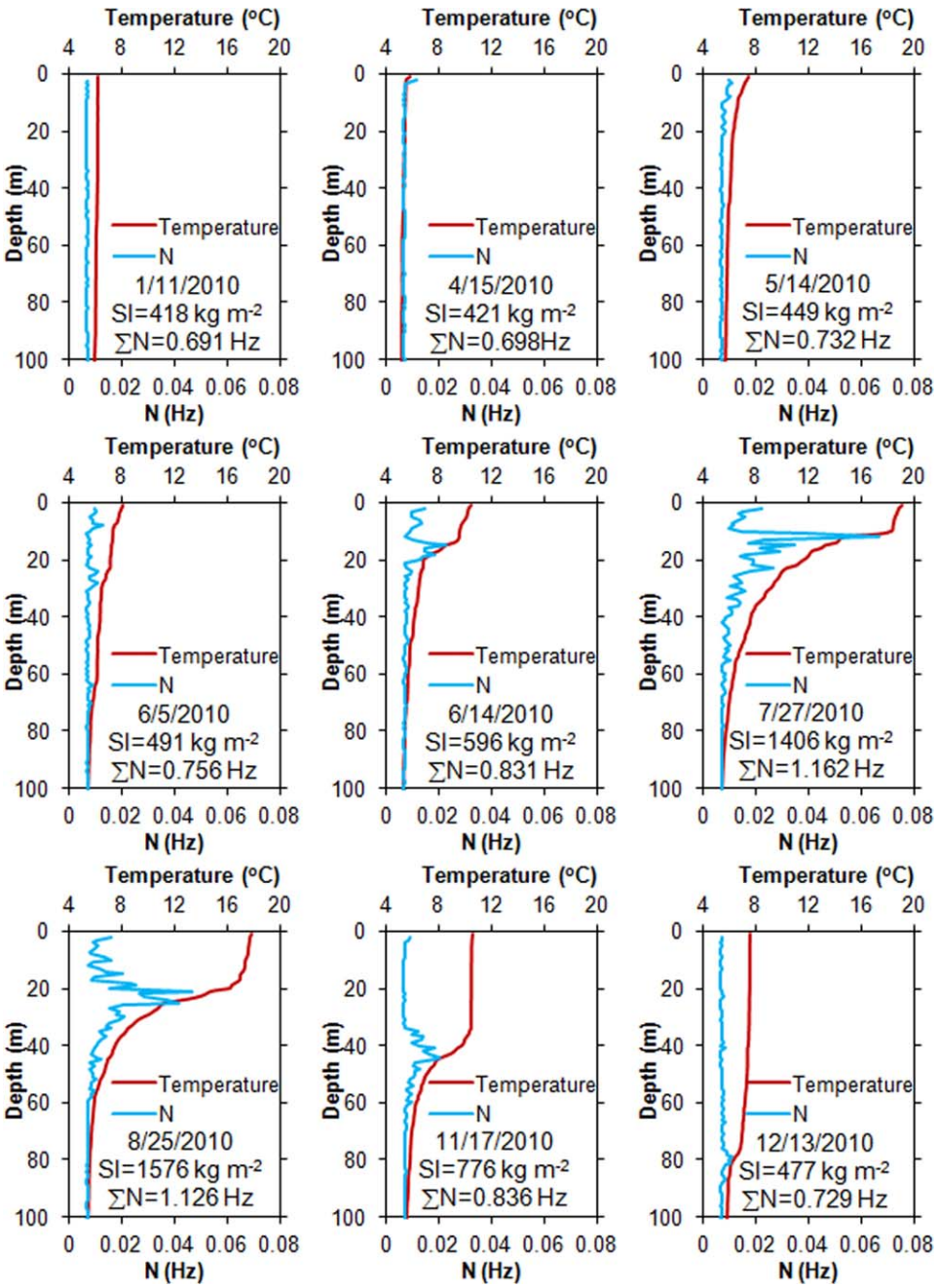

Fig. 4. Event based temperature profiles at 1 m interval measured using Seabird CTD profiler, buoyancy frequency (*N*) (i.e., stability in Hz) for every meter of water column, and SI for the upper 100 m water column during 2010. [Color figure can be viewed in the online issue, which is available at wileyonlinelibrary.com.]

Effect of continued warming on stratification

The length (days) and intensity (SI, kg/m^2) of lake stratification for the historical measurements (1968–2014) as well as the modeled GFDL A2 scenario (2001–2098) with 99% confidence intervals are shown in Figs. 6, 7, respectively. Note that GFDL A2 and B1 SI were calculated using the lake water temperature estimated by the lake model (Sahoo et al. 2010, 2013b; Sahoo and Schladow 2008) which utilizes the A2 and B1 projected air temperature, wind speed, solar radiation, dew point temperature and precipitation. The lake model also uses the hydrologic model predicted streamflows and associated pollutant (nitrogen, phosphorus and fine sediments) loadings into the lake. The archives containing GCMs' future projection for the IPCC Assessment (2007) contain daily outputs of temperature and precipitation, and for these other variables (i.e., radiative fluxes, winds, and

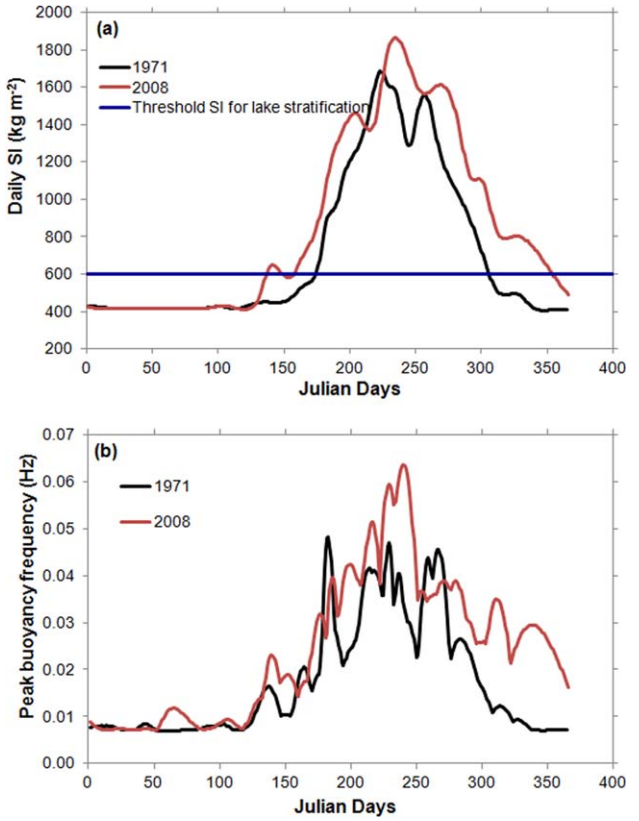

Fig. 5. Comparison of lake (**a**) SI and (**b**) peak *N* of year 1971 and 2008. Lake is considered stratified for SI-value and buoyancy frequency-value greater than 600 kg m^{-2} and 0.015 Hz, respectively. [Color figure can be viewed in the online issue, which is available at wileyonlinelibrary.com.]

humidity values) archives often are limited to certain period or monthly statistics. Thus, projected daily air temperature and precipitation matched well ($R^2 = 0.9$ and 0.7, respectively) with those of historical values (1950–1998); however, the projected downscaled downward longwave fluxes, surface-wind speeds, and downward solar radiation are very well correlated ($R^2 = 0.95$, 0.9, and 0.8, respectively) only when aggregated to monthly time scales (Dettinger 2013). In addition, annual air temperature in Fig. 6c shows that projected A2 and B1 annual air temperatures during 2001–2014 do not exactly overlap; rather the trend of projected A2 follows closely that of measured annual air temperature while trend of projected B1 annual air temperatures is opposite to that of measured annual air temperature during 2001–2014. Therefore, the modeled and measured lake stratification length (days) and intensity (SI, kg/m^2) during 2001–2014 do not overlap. The trends are such that the lengthening of stratification seasons under the A2 are almost a direct extension of the observed historical trend (in contrast to the slower lengthening projected under scenario B1). The linear regression line with very strong statistical correlation significance value (Mann-Kendall p-value < 0.0001) in Fig. 6a indicates that the length of stratification season may increase by 62 d in the entire 130-yr, measured and modeled dataset. However, the stratification season by the end of the century is projected to begin approximately 16 d earlier (Mann-Kendall p-value $= 7.46 \times 10^{-9}$) under the A2 scenario (Fig. 7, lower panel) and end about 22 d later (Mann-Kendall p-value $= 9.01 \times 10^{-10}$) between 2014 and 2098. While the date of peak stratification does not appear to vary much around a value of 240 (Julian date), the stratification season will begin 21 d earlier in case of GFDL A2 scenario and the end of the stratification season will be extended by 41 d (Fig. 7) during 1968–2098. These trends are supported by the trends of the historical dataset, which indicate the earlier onset of the spring stratification season and the delay in the onset of winter mixing. The magnitude of lake stratification in terms of SI (kg/m^2) in case of GFDL A2 scenario is found to be increased at a rate (3.025 kg/m^2/yr, Mann-Kendall p-value $= 1.05 \times 10^{-20}$) similar to those of historical dataset (Fig. 6d) when compared with the trends of historical 1968–1996 and projected 2001–2098. Until the late 1990s, the lake warming rate was considerably greater (approximately at 0.207°C/decade Fig. 2c), but a high number of deep mixing years during 1997–2011 (TERC 2015) have slowed the warming rate. Consecutive three warmer years (2012, 2013, and 2014 in Fig. 3) pulled the warming trend close to that of historical 1968–1996 (Fig. 2b,c).

The duration (days) of lake stratification for GFDL B1 scenario and historical records are shown in Fig. 6a. The length of the stratification season under the B1 scenario increases by approximately 12 d (Mann-Kendall p-value $= 0.0008$) between 2014 and 2098, which is proportionately lower than historical records. As B1 emissions stabilize and temperatures follow suit after 2050, lengthening of projected stratification durations slows. The magnitude of lake stratification in terms of SI (kg/m^2) in case of the GFDL B1 scenario is found to be increased at a much lower rate compared with those of historical dataset (Fig. 6c). In this study, the trends of duration (days) and intensity (SI, kg/m^2) of lake stratification in case of GFDL A2 scenario are found to be close to those of the historical dataset.

Discussion

Climate-driven warming trends have been observed in the historic hydro-meteorological data at Lake Tahoe. To better understand how the lake responds to current climatic forcing we presented trends of lake warming, lake stability magnitude, and increased stratification periods in Lake Tahoe. Commonly used stability indices, such as N^2, TSI, and RTR measure local stability (Fig. 4); whereas SSI and Hutchinson's SI estimate the idealized amount of energy required to mix the entire lake to a uniform temperature over the entire depth of the water column without the addition or subtraction of heat. However, surface water temperatures exhibit a rapid and direct response to climatic forcing in contrast to

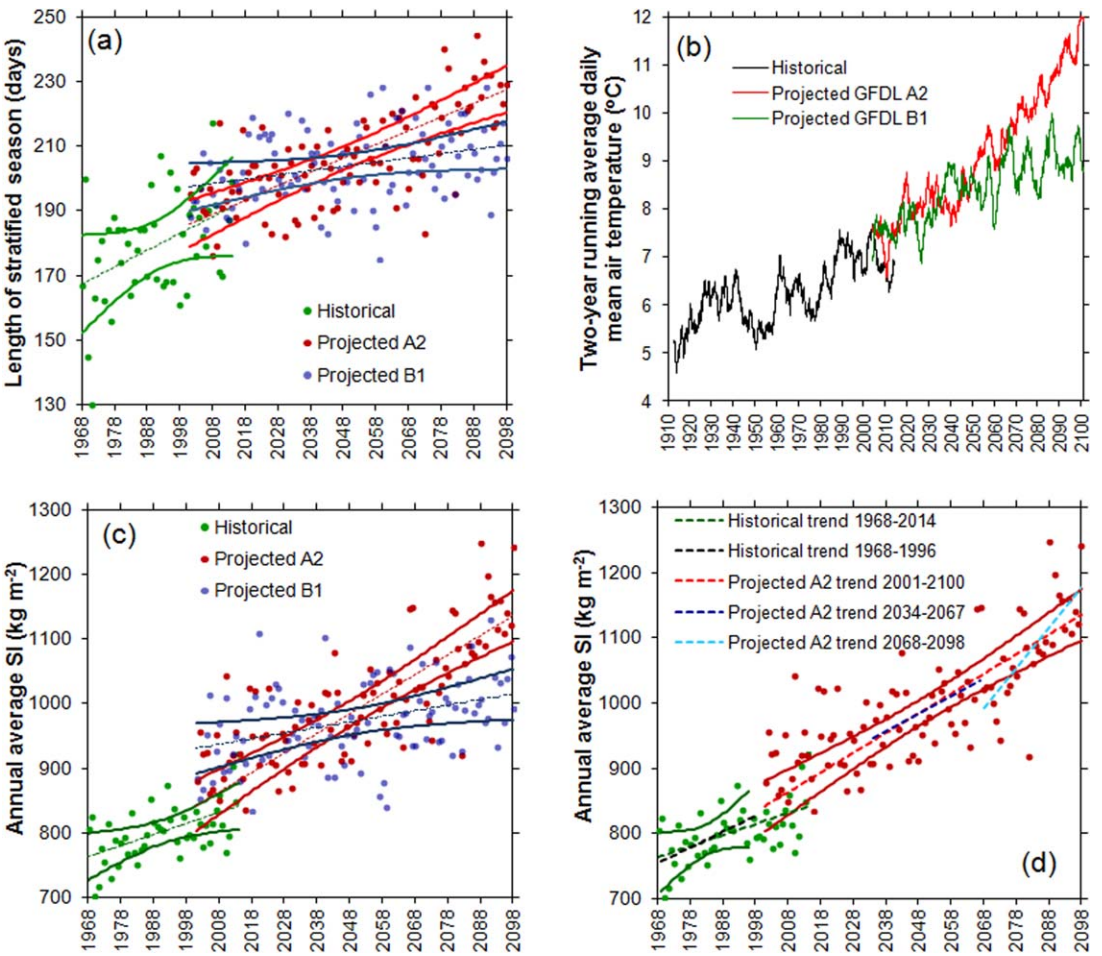

Fig. 6. (**a**) Length of stratification season in a year, (**b**) historical and projected daily average air temperature, (**c**) annual average SI (kg m^{-2}) in a year, and (**d**) annual average SI (kg m^{-2}) in a year. The solid lines in (**a**), (**b**), and (**d**) represent the 99% confidence intervals. The dashed lines in (**a**), (**b**), and (**d**) represent the linear regression trend lines. [Color figure can be viewed in the online issue, which is available at wileyonlinelibrary.com.]

hypolimnetic temperatures that exhibit a much more complex behavior, making epilimnetic temperature a useful indicator of climate change. The disadvantage of the using SSI for very deep lakes is that the rest of the water column overwhelms variations in stability of the upper stratified water column. As stratification in Lake Tahoe is observed in the upper 100 m (Fig. 4), we developed a simple stratification index (SI) to measure the stratification intensity and duration of the upper 100 m of the lake water column (Fig. 5). Because the SI is easier to produce and measure of Lake Tahoe stratification lengths accurately; it is more informative measure of lake stability than more commonly used indices.

Climate change is one of the biggest threats for Lake Tahoe's ecosystem. The climate models evaluated in the most recent IPCC Assessment (2007) shows a wide range of uncertainties regarding climate-change projections. In this study, we chose two scenarios A2 and B1, because scenario A2 is considered as a representative of middle of the road climate-change projections and B1 scenario is considered to be an optimistic scenario that results in much less climatic change and challenge than does the A2 scenario. As future climate is uncertain, these two scenarios will show the probable range of possible lake responses to climate change.

Climate change is evident at both regional and global scales (Cayan et al. 2008; Karl et al. 2015). Sahoo et al. (2011) documented the warming trends in the hydrometeorological dataset (1950–2007) of the Tahoe basin showing that minimum and maximum air temperatures have increased at 0.04°C/yr and 0.02°C/yr, respectively; timing of peak streams discharge due to snowmelting has shifted to earlier date at a rate of about 0.4 d/yr; and the percentage of total annual precipitation falling as snow has decreased by 15–20% (Coats 2010). As a result, the Lake Tahoe has become both warmer and more stable (Stewart et al. 2005; Schneider et al. 2009; Sahoo et al. 2011). In this study, it is found that length stratification duration has already increased more than 3 weeks during 1968–2014 and it is

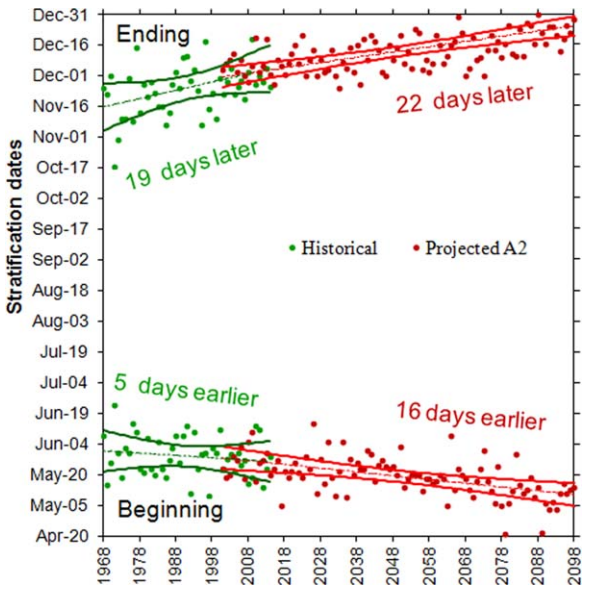

Fig. 7. The lake stratification dates in a year for historical and GFDL A2 SRES scenarios. The dashed lines show the best-fit linear regression trends. The solid lines represent the 99% confidence intervals. The Mann-Kendall *p*-values for historical stratification beginning and end dates are 0.398 and 0.004, respectively. The Mann-Kendall *p*-values for GFDL A2 stratification beginning and end dates are 7.46×10^{-9} and 9.01×10^{-10}, respectively. [Color figure can be viewed in the online issue, which is available at wileyonlinelibrary.com.]

projected to increase additional 38 d between 2014 and 2098 when modeled using the downscaled GFDL A2 scenario for the Lake Tahoe region. Similar to the increasing stratification period, lake stability under the A2 scenario is projected to increase at a rate of 3.025 kg/m^2/yr during 2014–2098 (1.8 times higher than the trend of 1968–2014, i.e., 1.662 kg/m^2/yr) (Fig. 6d). Figure 6d shows that lake stability under A2 during 2068–2098 is projected to increase at higher rate (6.191 kg/m^2/yr, i.e., 3.7 times higher than the trend of 1968–2014, i.e., 1.662 kg/m^2/yr). Increasing stability will require higher wind energy to initiate deep mixing.

Climatic warming of lake water will potentially result in lower DO concentrations (Blumberg and Di Toro 1990; Stefan and Fang 1994a,b; Fang and Stefan 2009; Palmer et al. 2014). Lake Tahoe epilimnion is relatively well mixed due to mixing energy induced from the wind. The epilimnion deepens during winter as surface waters cool and sink downward due to decreased air temperatures and solar radiation. The wind energy and intense cooling of winter storms determines how deeply the lake mixes. Mixing depth has profound impacts on lake ecology and water quality. Deep mixing brings available nitrogen and phosphorus to the surface, where they promote algae growth (Paerl et al. 1975). This process also transfers oxygen to deep waters, promoting aquatic life throughout the water column and in the surficial bottom sediments. Since mixing occurs due to the energy generated by wind and density-driven convection of surface water, the deepest mixing typically occurs in February–March (TERC 2015). Sahoo et al. (2011, 2013a) demonstrated that under modeled conditions of continued warming deep mixing (> 300 m) could cease entirely after 2065 for the GFDL A2 scenario. This is consistent with the increasing stability during 2068–2098 shown in Fig. 6d.

The projected increasing stability will require greater destabilizing energy from the meteorological forcing to initiate deep mixing. This is compounded by the reduced time over which the lake is not stratified in the upper 100 m. Simply put more energy is required in less time. The stratification period for Lake Tahoe typically starts in June, peaks in October and ends in November, although the lake does not mix to the bottom (a depth of 500 m) until February or March, and then only (on average) in one of four years. When the lake fails to completely mix, the bottom waters will not be replenished with oxygen and eventually dissolved oxygen concentrations at depths greater than 300 m will decrease to zero (Sahoo et al. 2013a). When this occurs, both soluble reactive phosphorus (SRP) and ammonium-nitrogen will be released from the anoxic sediments. Based on published results for SRP and ammonium release from anoxic Lake Tahoe sediment (Beutel 2000; Sahoo et al. 2013a), the annual loading of SRP under sustained conditions of lake stratification (no deep mixing) and anoxic sediments would be twice the current load from all other sources. Loading of ammonium under these conditions would increase the amount of biological available nitrogen that enters the lake by 25%.

The process of lake eutrophication, be it by natural processes or by contemporary increases in external nutrient loads, has long been understood to embody changing conditions that may include increased productivity, decreased clarity, highly variable dissolved oxygen and changing algal species (Wetzel 2003). Climatic eutrophication, while likely producing the same conditions, is induced by the direct and indirect effects of climate change. Such changes in lakes around the world are a likely outcome of continued atmospheric warming and the concomitant factors it produces. Other potential consequences can also be envisioned. With increasing hypolimnetic detention times, anaerobic decomposition may occur, leading to the accumulation and eventual release of methane. Deepwater anoxia will also significantly limit habitat availability for the lake's salmonid community, and at the same depths, oxygen concentrations could be inhospitable to the coldwater fishery (<6 mg/L) even earlier. The effect of climate change on the nutrient loading budgets and loss of coldwater fish habitat will have an extraordinary and long-lasting impact on the physical, chemical and biological ecology of Lake Tahoe. Finally, longer stratification seasons, with their resulting warmer lake water surface temperatures, will increase evaporation from the lake (Sahoo et al. 2013a). Sahoo et al. (2013a) projected climatic warming would drive the lake water surface level

down below the lake natural rim after 2085 for the GFDL A2 because of higher evaporation rate. This shifting balance will present a serious challenge for water managers. Climate-driven epilimnion warming has been found in many lakes (Adrian et al. 2009; Palmer et al. 2014). Although individual lake response to recent warming differs from lake to lake depending on the lakes' internal physical structures, morphometries, hydrological settings, and biota, long-term epilimnetic thermal structure changes represent good indicators of climate change because of the directness and sensitivity of their response to climatic forcing. However, published literatures show the use of conventional stability index SSI using the entire water column for lake stability estimate, which is not a good representation of lake response to climate change forcing.

Conclusions

Analysis of historical hydro-meteorological data shows that the Lake Tahoe stratification season and stratification intensity increased by approximately 24 d and at a rate of 16.62 kg/m^2/decade, respectively during 1968–2014. The simulated GFDL A2 and B1 results for Lake Tahoe show a continuation and intensification of the already observed trends. The time-length of stratification is projected to increase by 62 d by the end of 2098 relative to 1968 in case of GFDL A2 scenario, and is proportionately similar to historical records. The annual average lake stability under A2 scenario is projected to increase at 30.25 kg/m^2/decade during 2014–2098 and at higher rate during 2066–2098 (61.91 kg/m^2/decade) than the trend of 1968–2014. The consequences of this change to the vulnerable Lake Tahoe ecosystem will include exacerbation of existing water quality problems (e.g., reduced mixing, lower dissolved oxygen and/or development of anoxia in the hypolimnion, release of bio-stimulatory nitrogen and phosphorus) and water supply problems (e.g., increased lake surface temperature, higher evaporation rate) driven primarily by climate change.

The findings here, and the analytical approaches used, has potential application for projection and detection of the impacts of climate change on surface stratification, mixing regimes, ecosystem structure and function, and the consequences on ecosystem services in a lake. While the critical lake factors such as lengthening and intensifying stratification season are clearly measurable, the consequences have only been detected to date in the lake's changing algal species composition (Winder et al. 2009). However, model predictions support the notion that the most extreme manifestations, likely to be triggered by hypolimnetic anoxia and resulting consequences on ecosystems such as the process of climatic eutrophication, may only be a few decades away. There is little reason to believe such changes are limited to just Lake Tahoe. Rather, similar changes must be occurring in many other lakes and freshwater aquatic ecosystems worldwide.

References

Adrian, R., and others. 2009. Lakes as sentinels of climate change. Limnol. Oceanogr. **54**: 2283–2297. doi:10.4319/lo.2009.54.6_part_2.2283

Beutel, M. W. 2000. Dynamics and control of nutrient, metal and oxygen fluxes at the profundal sediment-water interface of lakes and reservoirs. Dissertation. Univ. of California Berkeley, Berkeley.

Blumberg, A. F., and D. M. Di Toro. 1990. Effects of climate warming on dissolved oxygen concentrations in Lake Erie. Trans. Am. Fish. Soc. **119**: 210–223. doi:10.1577/1548-8659(1990)119<0210:EOCWOD>2.3.CO;2

Cayan, D. R., E. P. Maurer, M. D. Dettinger, M. Tyree, and K. Hayhoe. 2008. Climate change scenarios for the California region. Clim. Change **87**: 21–42. doi:10.1007/s10584-007-9377-6

Chen, C. T., and F. J. Millero. 1986. Precise thermodynamical properties for natural waters covering only the limnological range. Limnol. Oceanogr. **31**: 657–662. doi:10.4319/lo.1986.31.3.0657

Coats, R. 2010. Climate change in the Tahoe basin: Regional trends, impacts and drivers. Clim. Change **102**: 435–466. doi:10.1007/s10584-10010-19828-10583

Coats, R., J. Perez-Losada, G. Schladow, R. Richards, and C. Goldman. 2006. The warming of Lake Tahoe. Clim. Change **76**: 121–148. doi:10.1007/s10584-005-9006-1

Delworth, T. L., and others. 2006. GFDL's CM2 global coupled climate models—part 1: Formulation and simulation characteristics. J. Clim. **19**: 643–674. doi:10.1175/JCLI3629.1

Dettinger, M. 2013. Projections and downscaling of 21st century temperatures, precipitation, radiative fluxes and winds for the Southwestern US, with focus on Lake Tahoe. Clim. Change **116**: 17–33. doi:10.1007/s10584-012-0501-x

Dufresne, J. L., and others. 2013. Climate change projections using the IPSL-CM5 Earth System Model: From CMIP3 to CMIP5. Clim. Dyn. **40**: 2123–2165. doi:10.1007/s00382-012-1636-1

Fang, X., and H. G. Stefan. 2009. Simulations of climate effects on water temperatures, dissolved oxygen, and ice and snow covers in lakes of the contiguous United States under past and future climate scenarios. Limnol. Oceanogr. **54**: 2359–2370. doi:10.4319/lo.2009.54.6_part_2.2359

Gardner, J. V., A. M. Larry, and J. H. Clarke. 1998. The bathymetry of Lake Tahoe, California–Nevada. US Geological Survey, Open-File Report 98-509. Available from http://tahoe.usgs.gov/bath.html

Hutchinson, G. E. 1957. A treatise on limnology, v. 1. Wiley.

Idso, S.B. 1973. On the concept of lake stability. Limnol. Oceanogr., **18**: 681e683.

Intergovernmental Panel on Climate Change (IPCC). 2007. Climate change 2007-The physical science basis. Available from http://www.ipcc.ch/ipccreports/ar4-wg1.htm

Jassby, A. D., C. R. Goldman, J. E. Reuter, and R. C. Richards. 1999. Origins and scale dependence of temporal variability in the transparency of Lake Tahoe, California-Nevada, Limnol. Oceanogr., **44**: 282–294.

Karl, T. R., and others. 2015. Possible artifacts of data biases in the recent global surface warming hiatus. Science **348**: 1469–1472. doi:10.1126/science.aaa5632

Koenigk, T., L. Brodeau, R. G. Graversen, J. Karlsson, G. Svensson, M. Tjernström, and K. Willén. 2013. Arctic climate change in 21st century CMIP5 simulations with EC-Earth. Clim. Dyn. **40**: 2719–2743. doi:10.1007/s00382-012-1505-y

Millero, F. J., C. T. Chen, A. Bradshaw, and K. Schleicher. 1980. A new high pressure equation of state for seawater. Deep-Sea Res. **27A**: 255–264. doi:10.1016/0198-0149(80)90016-3

Paerl, H. W., R. C. Richards, R. L. Leonard, and C. R. Goldman. 1975. Seasonal nitrate cycling as evidence for complete vertical mixing in Lake Tahoe, California-Nevada. Limnol. Oceanogr. **20**: 1–8. doi:10.4319/lo.1975.20.1.0001

Palmer, M. E., N. D. Yan, and K. M. Somers. 2014. Climate change drives coherent trends in physics and oxygen content in North American lakes. Clim. Change **124**: 285–299. doi:10.1007/s10584-014-1085-4

Pawlowicz, R. 2008. Calculating the conductivity of natural waters. Limnol. Oceanogr.: Methods **6**: 489–501. doi:10.4319/lom.2008.6.489

Read, J. S., and others. 2011. Derivation of lake mixing and stratification indices from high-resolution lake buoy data. Environ. Model. Softw. **26**: 1325–1336. doi:10.1016/j.envsoft.2011.05.006

Sahoo, G. B., and S. G. Schladow. 2008. Impacts of climate change on lakes and reservoirs dynamics and restoration policies. Sustainability Sci. **3**: 189–200. doi:10.1007/s11625-008-0056-y

Sahoo, G. B., S. G. Schladow, and J. E. Reuter. 2010. Effect of sediment and nutrient loading on Lake Tahoe (CA-NV) optical conditions and restoration opportunities using a newly developed lake clarity model. Water Resour. Res. **46**:1–20. doi:10.1029/2009WR008447

Sahoo, G. B., S. G. Schladow, J. E. Reuter, and R. Coats. 2011. Effects of climate change on thermal properties of lakes and reservoirs, and possible implications. Stoch. Environ. Res. Risk Assess. (SERRA) **25**: 445–456. doi:10.1007/s00477-010-0414-z

Sahoo, G. B., and others. 2013a. The response of Lake Tahoe to climate change. Clim. Change **116**: 71–95. doi:10.1007/s10584-012-0600-8

Sahoo, G. B., S. G. Schladow, and J. E. Reuter. 2013b. Hydrologic budget and dynamics of a large oligotrophic lake related to hydro-meteorological inputs. J. Hydrol. **500**: 127–143. doi:10.1016/j.jhydrol.2013.07.024

Sahoo, G. B., and S. G. Schladow. 2014. Estimation of heat and hydrologic budget of Upper Klamath Lake Oregon, USA using updated DLM-WQ Model. Water Resour. Manag. **28**: 1395–1414. doi:10.1007/s11269-014-0559-5

Schmidt, W. 1928. Über Temperatur and Stabilitätsverhaltnisse von Seen. Geographiska Annaler **10**: 145–177.

Schneider, P., S. J. Hook, R. G. Radocinski, G. K. Corlett, G. C. Hulley, S. G. Schladow, and T. E. Steissberg. 2009. Satellite observations indicate rapid warming trend for lakes in California and Nevada. Geophys. Res. Lett. **36**. doi:10.1029/2009GL040846

Stefan, H. G., and X. Fang. 1994a. Model simulations of dissolved oxygen characteristics of Minnesota lakes: Past and future. Environ. Manag. **18**: 73–92. doi:10.1007/BF02393751

Stefan, H. G., and X. Fang. 1994b. Dissolved oxygen model for regional lake analysis. Ecol. Modell. **71**: 37–68. doi:10.1016/0304-3800(94)90075-2

Stewart, I., D. R. Cayan, and M. Dettinger. 2005. Changes toward earlier streamflow timing across western North America. J. Clim. **18**: 1136–1155. doi:10.1175/JCLI3321.1

Tahoe Environmental Research Center (TERC), University of California Davis. 2015. Tahoe: State of the Lake Report 2015.

U.S. Global Change Research Program. 2009. Global climate change impacts in the United States. Available from http://nca2009.globalchange.gov/

Vallentyne, J. R. 1957. Principles of modern limnology. Am. Sci. **45**: 218–244. doi:A1957WE05500004

Wetzel, R. G. 2003. Limnology, 2nd ed. Saunders College Publishing.

Winder, M., D. E. Schindler, T. E. Essington, and A. H. Litt. 2009. Disrupted seasonal clockwork in the population dynamics of a freshwater copepod by climate warming. Limnol. Oceanogr. **54**: 2493–2505. doi:10.4319/lo.2009.54.6_part_2.2493

Yu, H., H. Tsuno, T. Hidaka, and C. Jiao. 2010. Chemical and thermal stratification in lakes. Limnology **11**: 251–257. doi:10.1007/s10201-010-0310-8

Acknowledgments

We acknowledge the foresight of Professor C. R. Goldman for the value he placed on the importance of a continuous long-term dataset and all his colleagues who have maintained this extensive record. In particular we thank Bob Richards and Brant Allen for directing the lake sampling program for the past 45 yr. We also thank Patty Arneson in her role as data archivist and QA/QC specialist. This work was partially supported by grant #08-DG-11272170-101 from the USDA Forest Service Pacific Southwest Research Station and the UC Davis Tahoe Environmental Research Center.

Submitted 13 March 2015
Revised 15 August 2015
Accepted 19 October 2015

Associate editor: John Downing